PERFORMANCE OF MAGNETIC-SUPERCONDUCTOR NON-CONTACT HARMONIC DRIVE FOR CRYOGENIC SPACE APPLICATIONS: SPEED, TORQUE AND EFFICIENCY MEASUREMENTS

Jose Luis Perez-Diaz (1), Efren Diez-Jimenez (1), Ignacio Valiente-Blanco (2), Cristian Cristache (2), Marco-Antonio Alvarez-Valenzuela 2, Juan Sanchez-Garcia-Casarrubios(2)

(1) Departamento de Teoría de la Señal y Comunicaciones, Universidad de Alcalá, 28871 Alcalá de Henares, Spain:jl.perezd@uah.es

(2) R&D department, MAG SOAR SL (www.magsoar.com), 28341, Valdemoro, Spain, Email:ivaliente@magsoar.com

ABSTRACT

Harmonic Drives are widely used in space mainly because of their compactness, large reduction ratio ad zero backlash. However, their use in extreme environments like in cryogenic temperatures is still a challenge. Lubrication, lifetime and fatigue are still issues under these conditions.

The MAGDRIVE project, funded by the EU Space FP7 was devoted to test a new concept of harmonic drive reducer. By using the magnetic distance force interactions of magnets and ferromagnetic materials, all the conventional mechanical elements of a Harmonic Drives (teeth, flexspline and ball bearings) are substituted by contactless mechanical components (magnetic gear and superconducting magnetic bearings). The absence of contact between any moving parts prevents wear, lubricants are no longer required and the operational life time is greatly increased. As the magnetic transmission is continuous there is no backlash in the reduction. MAG SOAR Company is already providing contactless mechanical components for space applications able to operate in a wide range of temperatures.

In this paper the tests results of a -1:20 ratio MAGDRIVE prototype are reported. In these tests successful operation at 40 K and 10-3 Pa was demonstrated for more than 1.5 million input cycles. A maximum torque of 3 Nm and efficiency higher than 75% at 3000 rpm were demonstrated. The maximum tested input speed was 3000 rpm -six times the previous existing record for harmonic drives at cryogenic temperature.

INTRODUCTION

Harmonic Drives (HD) are transmission mechanisms able to develop high ratios, providing a high positional precision, with relatively low weight/volume ratio, high torque capability and near zero backlash. Invented by Musser in 1955 [1] for aerospace applications, HD are currently widely used in robotics[2], [3], medical equipment, printing presses, vehicles and defense. They are also used in Space mainly because a good performance in terms of reduction ratio and good efficiency with respect to conventional gear trains [4][5]. Typically, the temperature operation range of HD in space is limited from -40°C to +100 °C [6], [7].

However, at very low temperatures, conventional mechanisms present severe tribological problems in bearings and teeth like cold spots, fatigue and wear [8], [9]. Only solid lubricants such as PFTE or MoS2 can be a solution at low temperatures [10],[11]. Nevertheless, for long life-time operation solid lubricants turn out not to be a very reliable solution and the decrease of the efficiency in the mechanism it is very significant.

Specifically, the application of HD mechanisms is limited by the severe drop of the efficiency at low temperature. For instance, the efficiency of conventional HD falls below 20% at temperatures below -40°C, even when using dry lubricants like the MAPLUB SH050a Grease [12].

Additionally, dry lubricants present grating, clutching, rapid wear out, instability of the friction coefficient, formation of cold weld centres and losses or decomposition at cryogenic conditions. This prevents conventional HD with dry lubricants from rotating faster than 500 rpm in the input axle. Moreover, fatigue associated to the intrinsic flexural functioning of the HD also limits their work life and efficiency at cryogenic temperatures.

The objective of the MAGDRIVE project, funded by the EU Space FP7, is to design, build and test a new concept of contactless harmonic drive. The limiting elements of conventional Harmonic Drives (teeth, flexspline and ball bearings) are substituted by contactless mechanical components (magnetic gear and superconducting magnetic bearings, [SMB]). The absence of contact between moving parts prevents wear, lubricants are no longer required and the operational life time is greatly increased. This also allows to keep a good efficiency independently of the temperature. Besides the cryogenic prototype, MAG SOAR Company is already providing contactless mechanical components for space applications able to operate in a wide range of temperatures. Combination of magnetic gears with conventional bearings seems to be the optimal solution for space applications. MAG SOAR are developing and offering optimized magnetic

Proc. '16th European Space Mechanisms and Tribology Symposium 2015', Bilbao, Spain, 23–25 September 2015 (ESA SP-737, September 2015)

harmonic drive to space industry.

However, in this work, precursor of the MAG SOAR company, it is presented the mechanical performance of the first absolute zero friction machine. The major advantages that contactless mechanical components provide are: no friction between rotatory elements (no power losses or heat generation by friction so increase of efficiency), no lubrication is needed (oil-free mechanisms and no lubrication auxiliary systems), reduced maintenance (no lubricant so no need of oil replacements), wider operational temperature ranges (no lubricant evaporation or freezing), overload protection (if overload occurs magnet simply slides but no teeth brake), through-wall connection (decoupling of thermal and electrical paths and environmental isolation), larger operative speeds (more efficient operative conditions), ultralow noise and vibrations (no contact no noise generation).. Typically contactless mechanical elements are used separately. In this work, different contactless mechanical components are combined to create for the first time an absolute zero friction machine.

In order to achieve a Technology Readiness Level (TRL) 5, a prototype was designed, built and tested at a temperature of 40 K and 10-3 Pa. Mechanical performance including maximum speed, speed ratio, efficiency, torque and load capability, accuracy and reversibility were characterized. A maximum torque of 3 Nm and efficiency higher than 75% at 3000 rpm were demonstrated

WORKING PRINCIPLE

The working principle of the MAGDRIVE is like that of the Nonius-Vernier motors as shown in Figure 1, as very similar to the one of a conventional harmonic drive.

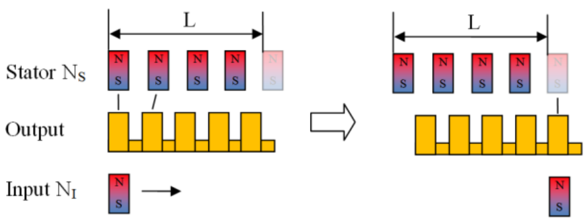

Figure 1. Scheme of the MAGDRIVE mesh principle.

The elementary mesh unit of a MAGDRIVE is composed of a stator provided with *ns* permanent magnet teeth uniformly distributed along a length *L*, a moving part (output) with *no* teeth made of soft magnetic material, and, finally, a single permanent magnet as an input. The condition for this to be an elementary mesh unit is that |*no*-*ns*| = *1*, as shown in Figure 1.

Displacement of the input tooth parallel to the length makes the output teeth magnetize and align, one by one, with the stator teeth. In this way, when the input moves along a length *L*, the output moves *L/no*. Therefore, the reduction of this movement will be *i* = *1/no* provided *no* is greater than *ns*. The ratio will be *i* = −*1/no* if *no* is smaller than *ns*.

Several elementary reduction units can be repeated *N* times along a circumference in order to build a coaxial gear of the same ratio *i*. In this case, there will be *Ns* = *N·ns* teeth in the stator, *No* = *N·no* teeth in the output, and *N* = *Ns-No* teeth in the input member. The reduction ratio for the coaxial gear can be also calculated as:

$$i = \frac{N_O - N_S}{N_O} \qquad (1)$$

This formula is valid for both positive and negative ratios. Both linear and rotational reductions are possible.

Additionally, like in any other kind of mechanism, a kinematic inversion can also be taken exchanging the roles of "input", "output", and "stator" (or mechanical ground).

In MAGDRIVE a rotational reduction, like in an harmonic drive, of prototype was designed comprising two elementary units with 42 teeth in the stator, 40 teeth in the output obtaining a reduction ratio of i = -20 (reversal of the rotation sense) as it is shown in figure 2.

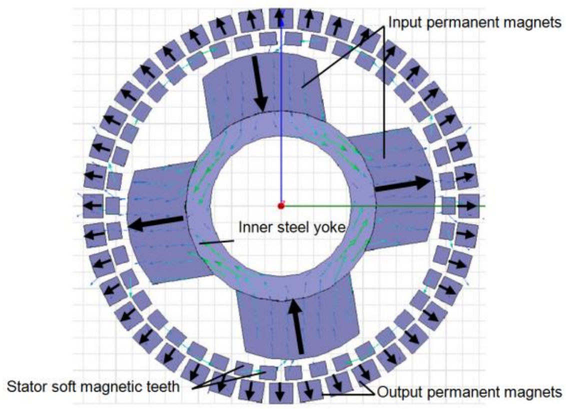

Figure 2. Magnetic configuration of MAGDRIVE prototype.

In the MAGDRIVE prototype the external ring was taken as output and the intermediate ring was taken as the stator. It was designed considering large airgaps between rotatory parts: 1 mm between output-stator and 2 mm between input and stator.

DESIGN AND MANUFACTURING

Mechanical Design

The design of the MAGDRIVE prototype is shown in next figure 3. The system is composed of a centered magnetic harmonic drive whose corresponding floating axles are supported by two pairs of superconducting magnetic bearings.

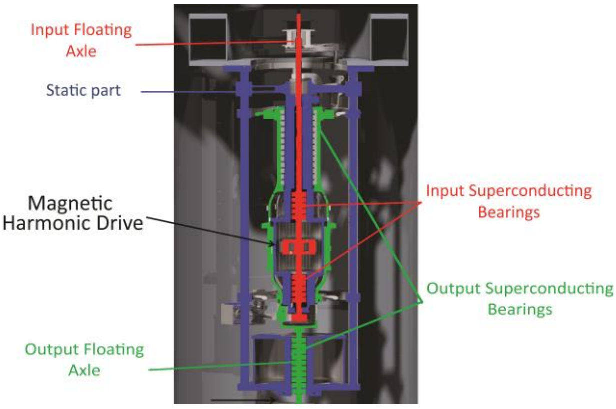

Figure 3. Mechanical design MAGDRIVE prototype.

Rotatory parts of the magnetic gear have instability of the permanent magnet rotors that impose a stiffness requirement for the bearings that hold the gears. Of course, the weight of each axle must be supported so an axial load appears. The requirements of radial and axial stiffness were deeply analyzed because they were critical for the design of the superconducting magnetic bearings, whose stiffness is much lower than a conventional mechanical ball bearing.

Recently, it has been explored different shapes, sizes and combination of magnet-superconductor in order to obtain more stable levitation positions [13]–[18]. There are some models that are useful to describe this interaction and that can be applied in finite elements programs as it is commonly used in mechanical engineering [19]–[21]. Some other parameters as the force relaxation or the rotation losses have to be considered from the point of view of the mechanical engineer for an adequate design of the SMB [22]–[25]. A full mechanical experimental characterization of the mechanical properties of the SMB was done [25]. SMB maximum axial and radial load, stiffness and force relaxation were characterized. Then, the total length of the SMB for input and output was defined in order to fulfill the requirements given by the magnetic gear instability analysis.

The required radial stiffness also depended on the arm-distance to the magnetic gear position, figure 2. The mechanical requirements for the input axle were 50 N/mm of radial stiffness and 14.5 N of axial load (weight). The requirements for the output were 110 N/mm of radial stiffness and 69 N of axial load. In order to prevent unbalance of the axles due to its total weight, it was decided to place the whole mechanism in vertical position.

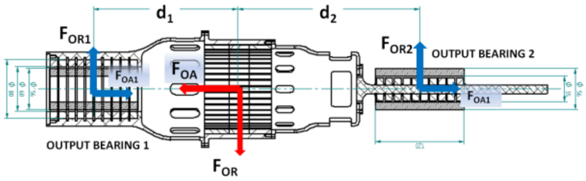

Figure 4. Superconducting magnetic bearing output design.

SMB were designed considering YBaCuO as superconducting material and NdFeB N50 as permanent magnet. The airgap between static and rotatory parts was 2 mm for input axle and 1 mm for output axle.

A safety factor of 2 was considered in the final design of the SMB. This implies larger SMB elements (60 mm for input and 120 mm for output ones). Although MAGDRIVE SMB were oversized for safety reasons, SMB, in general have much lower stiffness and load capacity than a mechanical ball bearing one. On the other hand, they do not have any friction or wear even at low temperature, and as explained that was the reason for their selection.

Other aspects like thermal management, sensors, and cooling systems were also critical for the design of the prototype. The prototype operational temperature was aimed to be 60 K. In order to get such a low temperature, two independent cooling systems were considered: two liquid nitrogen (LN2) reservoirs and a cryocooler of 48 W at 77 K.

The critical temperature of YBaCuO is 90 K. This means that all the superconductors have to be below 90 K to behave as superconducting material. Therefore, all superconducting bulks were placed in the static part, directly in conduction to the cryocooler or LN2 reservoirs.

The two floating axles, as shown in Figure 3, were held by a launch-lock system until the system reached the target temperature. Once the temperature was low enough, the launch-lock would open and they would be free to float in the vacuum. Similar concepts for launch-lock systems have been used in several devices . With the axles floating in a high vacuum, the only possible heating source would be radiation. Since the radiated areas of the floating axles were small, radiation was considered negligible and, therefore, the temperature of the floating axles in operation was expected to be close to the one just before release while testing.

Manufacturing

It is essential for the correct operation of the gear that all the magnetic parts are aligned and uniform in respect to each other. The geometrical tolerances for the magnet dimensions were measured from +0.0 to +0.1 mm for each direction. Thus, the positioning of the magnets had to be done with the same or better precision (±0.05 mm precision in the positioning inside their housings).

SmCo magnets do not have any coating by default, so it was necessary to apply a coating (in this case, Stycast Epoxy) in order to prevent any magnetic chips coming from the magnet.

The parts were assembled in a vertical configuration. Four aluminum columns were attached to the bottom LN2 deposit. This deposit was established as the reference plane; from there, all the different elements were guided through the aluminum columns and placed into the right height, as shown in Figure 5. Some special tools were manufactured for inserting each subassembly in the right position. The assembly sequence was followed according to the designed procedure.

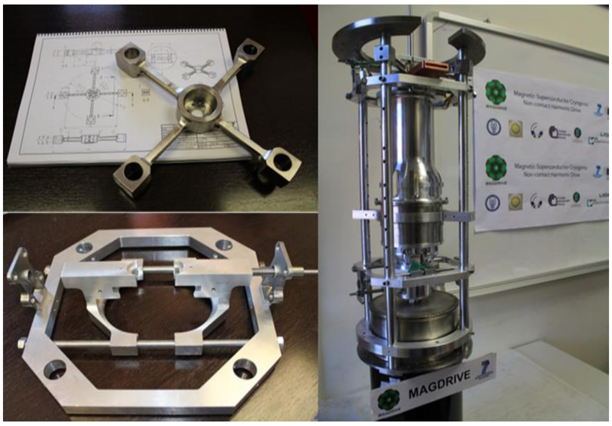

Figure 5. Structural connection (top-left), launch lock mechanism (bottom left) and MAGDRIVE assembled (right).

MECHANICAL TESTS

The prototype was integrated in the thermal-vacuum chamber, shown in Figure 6. It was connected to an upper LN2 tank acting as a second cold plate and the cryocooler finger was also connected to the static part of the prototype. The LN2 thermal circuit was used to cool down all the surrounding and external radiation foil and the cryocooler was used to cool down the superconducting bulks directly. Both systems were not connected between themselves.

Figure 6. MAGDRIVE integrated in the vacuum chamber.

Sensing system and vacuum chamber

The thermal-vacuum chamber and all the cooling and vacuum systems were adjusted and prepared for the operational test, shown in Figure 7. The chamber is a 304 stainless steel cylinder with a 1 m height and a 650 mm diameter, having a top and bottom flange with four lateral optical windows. The vacuum system is composed of a turbomolecular pump able to reduce the inner pressure below 10−3 Pa. The cooling system is composed of two LN2 tanks fed by a LN2 dewar with a 100 L capacity, and a cryocooler DE-104 from ARS Company with a 48 W cooling capacity at 77 K of the cold finger, able to reach 20 K. The chamber is provided with two endoscopic webcams to record video and picture inside the chamber.

The mechanical power was provided by an AC motor and a brake, installed in the top and bottom flange. Magnetomechanical feed-through were used for running through the mechanical power through the chamber flanges to the MAGDRIVE prototype.

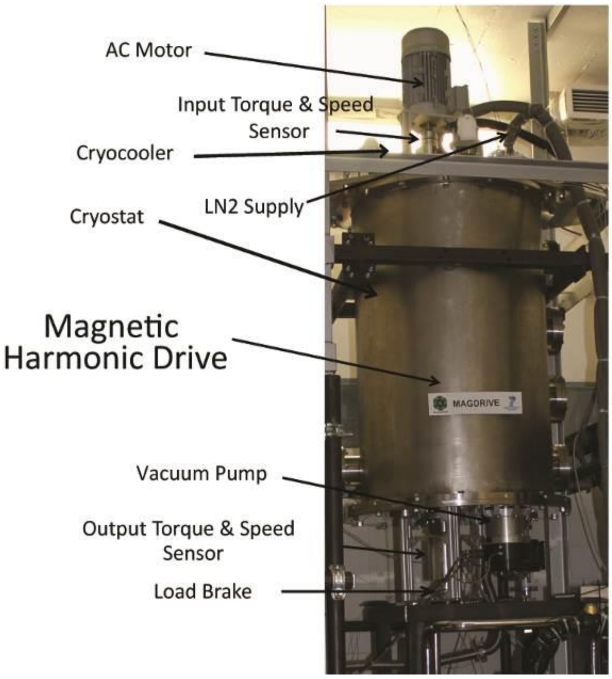

Figure 7. External assembly of the test.

The whole sensing system was composed of different kinds of sensors. The sensors installed externally were: input and output torque and speed sensors as shown in figure 7

Internally, input and output rotation and position contactless sensors were specifically constructed in order to measure the position of the floating axles. Additionaly, six inner temperature sensors in the static part, and four magnetic field sensors all along the height were installed in order to characterize thermal and magnetic behavior as shown in figure 8. Besides to those main sensors, some secondary sensors were added for the temperature control system: three temperature sensors and two level detectors for the LN2 deposits.

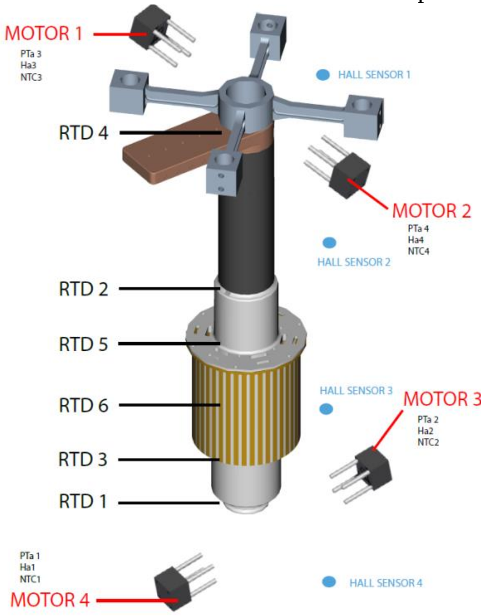

Figure 8. Internal location of the temperature and magnetic field sensors.

The output and input torque/speed sensors were two DATAFLEX 16-10 from KTR Company. The temperature sensors were PT-111 model from Lakeshore. The temperature control system sensors were composed of PTC sensors and a proportional-integral-derivative (PID) controller. The magnetic field sensors were HGCA-3020 model from Lakeshore. All the sensors were monitored by a PXI model system from National Instruments.

Vacuum and thermal cycles

Initially 5 thermal-vacuum cycles (T-V cycle) were done in order to check the proper temperature behavior. The last T-V cycle, just before the start of the dynamic tests, is shown in figure 9. The cooling system took almost two days to reach the needed temperature for the superconductors to be operative (< 90 K). However, this long time only applied for the bottom input SMB whose thermal path was very large and thin. Most of the prototype mass was well below 60 K in about 12 hours.

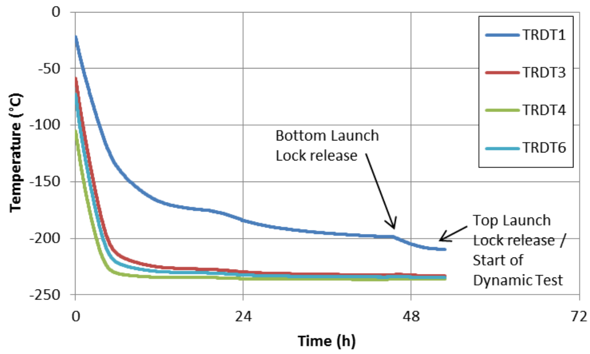

Figure 9. Cool down process.

The vacuum reached before starting the dynamic test was 3·10-3 Pa. Vacuum levels with time are shown in figure 10.

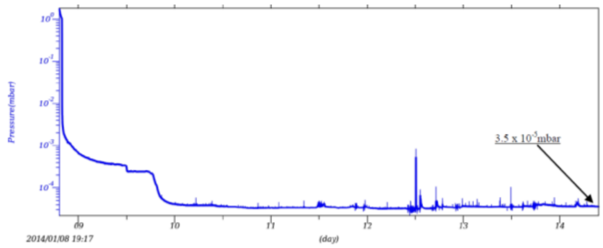

Figure 10. Vacuum levels in respect to time.

All the test shown next were done at this temperature and vacumm levels.

Speed and reversibility test

Speed of the input and output axles was registered. The AC two-pole motor accelerated the input axle until its maximum of 3000 rpm. The results of the measurement are shown in Figure 11.

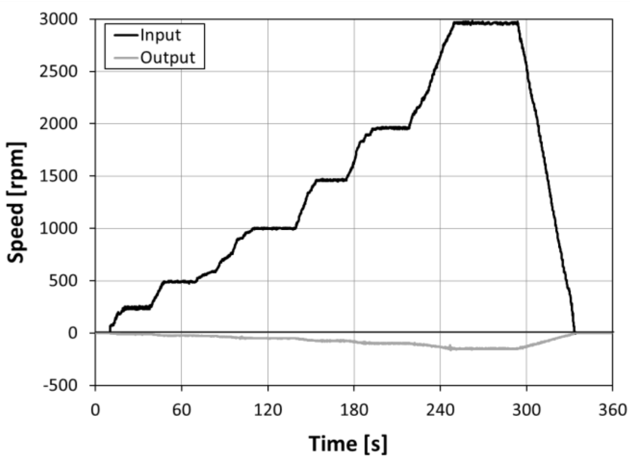

Figure 11. Input and output speed measurement.

In Figure 11, it can be observed the reduction and inversion of the speed in the output shaft in respect to the speed of the input. The reduction ratio calculated for all the speeds was -20, as expected from the design. The maximum speed achieved in the input axle was that of the AC motor, 3000 rpm. It is the first time that a HD can operate at this high an input speed in these temperature and vacuum conditions. A HD operating in cryogenic temperatures, moving faster than 500 rpm in the input axle, has never been registered before.

The reversibility of the systems (change of rotation sense) was tested with several inversions of the rotation sense with a maximum input speed of 500 rpm. The reversibility test measurements are shown in figure 12.

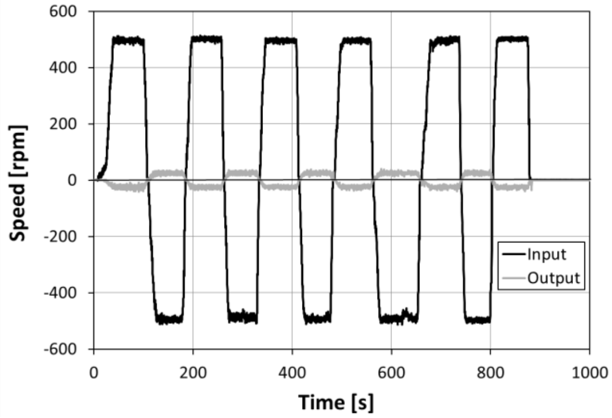

Figure 12. Reversibility of MAGDRIVE.

The prototype behave correctly for sudden changes in the rotation sense.

Load test

The maximum transmissible torque was measured by loading the external brake and transmitting the load through the magnetic couplings inside the chamber. The output torque measurements are shown in Figure 13.

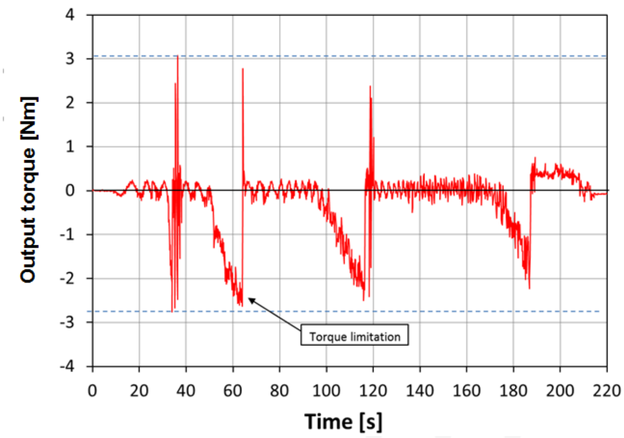

Figure 13. Output torque measurement.

The maximum transmissible torque was rated in 3 Nm, which gives a torque density of around 25 kNm/m3. Although the torque and corresponding torque density are low for practical applications, they correspond properly with the Finite Element Method (FEM) model results validating them. Torque capability can be easily improved by reducing air gaps (too conservative), using NdFeB magnets (caring about the spin reorientation transition), and optimizing shapes and sizes of the teeth as stated in next section.

Efficiency test

One of the major advantages of contactless operation of mechanical systems is that there are no power losses generated by friction. It is well know that friction loosse are predominant in any HD and that they are extremely high when operating at cryogenic temperatures. MAGDRIVE does not suffer any of these drawbacks beacause all the friction elements were substituted by contactless mechanical elements. On the other hand MAGDRIVE, as it is based in rotating magnetic field, there are eddy current losses. It is very important the adequate selection of the surrounding materials in order to reduce this power losses.

The efficiency of the power transmission was measured at different speeds in the cryogenic environment. The results are shown in figure 13.

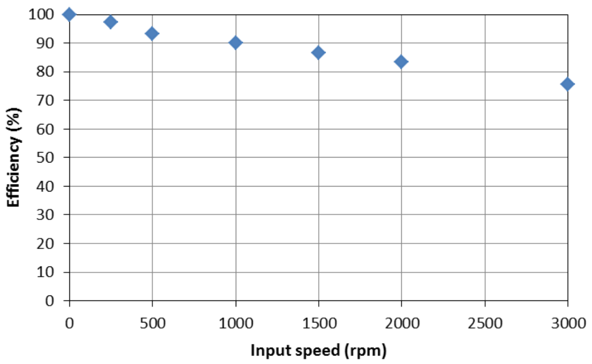

Figure 13.Efficiency of the system operating at 40 K.

The efficiency is almost 100 % at low speeds. At higher speeds the efficiency decreases. At the maximum speed 3000 rpm the efficiency was measured in 75%. The decrease of efficiency behaves linearly with the speed since the eddy current generation behaves quadratically with the speed. Although there is a decrease of the efficiency at 500 rpm (92%), the value is much higher than any other HD having operated at this temperature and speed. The value of the efficiency operating at 3000 rpm (75%) is the first time that is obtained, so no comparison can be done.

NEW MAGSOAR DEVELOPMENTS

MAG SOAR SL company was created as a spin-off company from the MAGDRIVE results. One of its main objectives is to turn magnetic harmonic drives useful for a wide range os space applications in different temperature regimes. A new invention of a company permit to foresee the wide application of magnetic harmonic drives in space applications.

MAG SOAR has obtained recently a contract from ESA inside the ITI program wherein the objetive is to increase significantly the torque density and specific torque of the magnetic gear in order to make them competitors of conventional HD in terms of torque with the extra advantages due to the lack of contact in the teeth and using conventional bearings.

The design results of this activity, started in april 2016, are very promising having demonstred torque densities of almost 150 kNm/m3 and 20 Nm/kg for reduction ratios of more than 1:100.

CONCLUSIONS

A radically different concept of HD was demonstrated operating at cryogenic temperatures. A MAGDRIVE was successfully designed, built, and tested at 40 K and 10−3 Pa. The performance test results are summarized in Table 1.

In this paper, the tests results of a −1:20 ratio MAGDRIVE prototype are reported. In these tests, successful operation at 40 K and 10−3 Pa was demonstrated for more than 1.5 million input cycles. A maximum output torque of 3 Nm and an efficiency of 75% were demonstrated. The maximum tested input speed was 3000 rpm, which is six times the previous existing record for HD at a cryogenic temperature.

Table 1. Performance test results of the MAGDRIVE prototype.

Parameter	Value
Reduction ratio	−1:20
Maximum input speed	3000 rpm
Maximum output torque	3 Nm
Torque density (without SMB and cooling systems)	25 kNm/m^3
Specific torque (without SMB and cooling systems)	7 Nm/kg
Weight of magnetic gear	428 g
Full prototype weight (SMB + sensors)	15 kg
Operational test temperature	40 K
Operational vacuum pressure	3×10^{-3} Pa
Lifetime (input cycles number)	1.5 million

MAG SOAR has obtained recently a contract from ESA inside the ITI program and the design results of this activity, started in april 2016, are very promising having demonstred torque densities of almost 150 kNm/m3 and 20 Nm/kg for reduction ratio of more than 1:100, using conventional mechanical bearings. This results permit to foresee the wide application of magnetic harmonic drives in space applications.

ACKNOWLEDGEMENTS

The research leading to these results has received funding from the European Community's Seventh Framework Programme ([FP7/2007–2013]) under grant agreement n° 263014. The FP7 MAGDRIVE project (www.magdrive.eu) is a cooperation project inside the Space program of the European Commission. Seven partners have participated: Universidad Carlos III de Madrid (Mechanical Engineering department), Università di Cassino e del Lazio Meridionale (LAMIA group), CNR (Istituo SPIN), CAN Superconductors, BPE e.K., LIDAX ingenieria S.L., and the Faculdade de Ciencias da Univerisdade de Lisboa (SIM lab). Special acknowledgment to Fernando Serrano, workshop technician at UC3M.

REFERENCES

[1] C. W. Musser, "Strain Wave Gearing," 2906143, 1955.

[2] C. Kennedy and J. Desai, "Modeling and control of the Mitsubishi PA-10 robot arm harmonic drive system," *IEEE/ASME Trans. MECHATRONICS*, vol. 10, no. 3, pp. 263–274, 2005.

[3] J. Sensinger and R. Weir, "Improved torque fidelity in harmonic drive sensors through the union of two existing strategies," *IEEE/ASME Trans. MECHATRONICS*, vol. 11, no. 4, pp. 457–461, 2006.

[4] Z. Hui, Z. Jun, S. Rui-Peng, and H. Hong, "Tungsten containing hydrogenated DLC coatings on grease lubricated harmonic drive gear for space application," in *14th European Space Mechanisms and Tribology Symposium*, 2011.

[5] J. Schmidt and M. Schmid, "LIFE TEST OF AN INDUSTRIAL STANDARD AND OF A STAINLESS STEEL HARMONIC DRIVE," *14th Eur. Sp. Mech. Tribol. Symp.*, 2011.

[6] INTA, "Antenna pointing mechanism for ESA Envisat polar platform." .

[7] ESA, *SENTINEL- 2*. 2012.

[8] Y. L. Ostrovskaya, T. Yukhno, G. Gamulya, Y. V. Vvedenskij, and V. Kuleba, “Low temperature tribology at the B. Verkin Institute for Low Temperature Physics & Engineering (historical review),” *Tribol. Int.*, vol. 34, no. 4, pp. 265–276, Apr. 2001.

[9] A. Trautmann, C. R. Siviour, S. M. Walley, and J. E. Field, “Lubrication of polycarbonate at cryogenic temperatures in the split Hopkinson pressure bar,” *Int. J. Impact Eng.*, vol. 31, no. 5, pp. 523–544, May 2005.

[10] G. Theiler, T. Gradt, and P. Klein, “Friction and wear of PTFE composites at cryogenic temperatures,” *Tribol. Int.*, vol. 35, pp. 449–458, 2002.

[11] N. Fleischer, M. Genut, L. Rapoport, and R. Tenne, “New nanotechnology solid lubricants for superior dry lubrication,” in *Proceedings of the 10th European Space Mechanisms and Tribology Symposium*, 2003, pp. 65 – 66.

[12] ESR Technology, *Space Tribology Handbook*. 2012.

[13] I. Valiente-Blanco, E. Diez-Jimenez, and J. L. Perez-Diaz, “Alignment effect between a magnet over a superconductor cylinder in the Meissner state,” *J. Appl. Phys.*, vol. 109, p. 07E704, 2011.

[14] E. Diez-Jimenez and J. L. Perez-Diaz, “Foundations of Meissner Superconductor Magnet Mechanisms Engineering,” in *Superconductivity - Theory and Applications*, 2011, pp. 153–172.

[15] E. Diez-Jimenez and J. Perez-Diaz, “Flip effect in the orientation of a magnet levitating over a superconducting torus in the Meissner state,” *Phys. C Supercond.*, vol. 471, no. 1–2, pp. 8–11, 2011.

[16] E. Diez-Jimenez and B. Sander, “Tailoring of the flip effect in the orientation of a magnet levitating over a superconducting torus: Geometrical dependencies,” *... C Supercond.*, vol. 471, no. 7–8, pp. 229–232, 2011.

[17] J. L. Perez-Diaz, E. Diez-Jimenez, I. Valiente-Blanco, and J. Herrero-de-Vicente, “Stable thrust on a finite-sized magnet above a Meissner superconducting torus,” *J. Appl. Phys.*, vol. 113, no. 6, p. 063907, 2013.

[18] E. Diez-Jimenez, I. Valiente-Blanco, and J. . Perez-Diaz, “Superconducting Sphere and Finite-Size Permanent Magnet: Force, Torque, and Alignment Effect Calculation,” *J. Supercond. Nov. Magn.*, vol. 26, no. 1, pp. 71–75, Jul. 2012.

[19] E. Diez-Jimenez, J. L. Perez-Diaz, and J. C. Garcia-Prada, “Mechanical method for experimental determination of the first penetration field in high-temperature superconductors,” *IEEE Trans. Appl. Supercond.*, vol. accepted, 2011.

[20] E. Diez-Jimenez, J. L. Perez-Diaz, and C. Castejon, “Finite element algorithm for solving supercondcuting Meissner repulsion forces,” *I.R.E.M.E.*, vol. 4, no. 6, pp. 673–675, 2010.

[21] E. Diez-Jimenez, J. L. Perez-Diaz, and J. C. Garcia-Prada, “Local model for magnet–superconductor mechanical interaction: Experimental verification,” *J. Appl. Phys.*, vol. 109, no. 6, p. 063901, 2011.

[22] C. Navau and A. Sanchez, “Stiffness and energy losses in cylindrically symmetric superconductor levitating systems,” *Supercond. Sci. Technol.*, vol. 15, no. 10, pp. 1445–1453, Oct. 2002.

[23] Y. Qin and X. Hou, “Influence of maglev force relaxation on the forces of bulk HTSC subjected to different lateral displacements above the NdFeB guideway,” *Phys. C Supercond.*, vol. 471, no. 3–4, pp. 118–120, Feb. 2011.

[24] Z. Xia, Q. Y. Chen, K. B. Ma, C. K. McMichael, M. Lamb, R. S. Cooley, P. C. Fowler, and W. K. Chu, “Design of superconducting magnetic bearings with high levitating force for flywheel energy storage systems,” *IEEE Trans. Appiled Supercond.*, vol. 5, no. 2, pp. 622–625, Jun. 1995.

[25] I. Valiente-Blanco and E. Diez-Jimenez, “Characterization and Improvement of Axial and Radial Stiffness of Contactless Thrust Superconducting Magnetic Bearings,” *Tribol. Lett.*, vol. 54, pp. 213–220, 2014.